INKJET-PRINTED CHEMIRESISTIVE SENSOR ARRAY WITH INTEGRATED HEATER

[1]Vojtěch POVOLNÝ, [1]Alexandr LAPOSA, [1]Jiří KROUTIL, [1]Pavel HAZDRA

[1]Faculty of Electrical Engineering, Czech Technical University in Prague, Prague, Czech Republic, EU,
povolvoj@fel.cvut.cz

https://doi.org/10.37904/nanocon.2024.5012

Abstract

An inkjet-printing method was used to fabricate a flexible gas sensor. This fabrication method is characterized by low material consumption, a fast design-to-fabrication process, and low fabrication cost. Due to these properties, this technology is increasingly popular in the fabrication of electronic circuits and devices. Gas sensors are devices generally used to detect the presence or, in more complex solutions, to measure the concentration of various gases. The fabrication technology and materials used determine sensor properties such as sensitivity, selectivity, repeatability, and stability for applications in general or industrial environments. In this research, we present the design preparation, fabrication, and characterization of the inkjet-printed gas sensor. The structures are based on silver nanoparticle ink and dielectric ink. The structures are printed on a flexible substrate and sintered using intense pulsed light and UV light, respectively. The printed sensors consist of an interdigital electrode (IDE) structure, a dielectric separation layer, and a heater pattern. The IDE structure is printed on the dielectric layer, which separates the heating and sensing structures. As a sensing layer, polyaniline (PANI) is drop-cast onto the IDE sensor structures. The inkjet-printed sensor was characterized based on its response to humidity and a test gas.

Keywords: Inkjet, gas sensor array, PET, IPL, microheater

INTRODUCTION

Monitoring of gaseous substances is crucial in many fields, such as industry, aviation, agriculture, healthcare, defense, and environmental monitoring [1], [2]. In response to meet the demand for sensors, a wide range of sensors, including metal oxide and conductive organic polymer-based devices, has been under intense research focus [3]. Flexibility, cost-effectiveness, light weight, and the ability to operate at room temperature are the key features that make chemical gas sensors based on polypyrrole (PPy), polyaniline (PANI), and poly(3,4-ethylene-dioxythiophene) (PEDOT) highly attractive [4]. Conducting polymers, as a class of organic materials, can be synthesized by chemical and electrochemical methods using a range of monomers in both aqueous and non-aqueous media [1]. Moreover, they provide a broad range of applications, such as energy storage [5]–[7], optoelectronic devices [8], and sensing of different gases and vapours like methanol, ethanol, acetone, benzene, NO, NO2, SO2, H2S, and some other toxic gases and vapours [9], [10].

Inkjet printing is a popular manufacturing technology today. It has gained popularity due to its low manufacturing costs, compatibility with a wide range of flexible and rigid substrates, low-temperature production process, and ease of use [11]. A wide range of electronic structures and devices can be produced with this technology, such as polymer light-emitting diodes (PLEDs) [12], nanoparticle MEMS (Micro Electro Mechanical Systems) [19], or chemiresistive gas sensors [14].

In this work, we report on the preparation of an inkjet-printed gas sensor matrix on a flexible substrate. We discuss the fabrication process, sensor's response to the detected gas, and the influence of temperature on the sensor's response.

1. MATERIALS AND METHODS

1.1. Substrate and ink

A combination of two inks was used to fabricate the presented gas sensor. For the preparation of the conductive part of the sensor, silver nanoparticle ink (ANP Silverjet DGP-40LT-15C, particle size <50 nm, solid content 35%, and resistivity 11 μΩ·cm) was used. A dielectric ink (Dycotec DM-INI-7003, Dycotec Materials Ltd, UK; volume resistivity $1.4 \cdot 10^{14}$ Ω·cm, UV curing wavelength 380 nm, UV curing energy 500 mJ·cm^{-2} – 1000 mJ·cm^{-2}) served as the isolation layer. Polyethylene terephthalate (PET) was selected as a suitable substrate for the fabrication of the sensor due to its advantageous properties for printed electronics, such as flexibility, dimensional stability, chemical resistance, and cost-effectiveness. As a result, PET is popular for low-cost, low-temperature applications in inkjet printing fabrication [15].

The printing conditions were set as follows: the metal structures were printed with the cartridge (DMC 11610), which was heated to 35 °C, at a resolution of 1016 dpi and a jetting frequency of 2 kHz. The substrate temperature was maintained at 40 °C. High-intensity pulsed light (Xenon X-1100, Xenon Corporation, USA) was used to sinter the printed structures, with a radiant energy of up to 9 J·cm^{-2} per broad-spectrum light pulse. Two flashes with durations of 300 μs and 200 J, with a 60-second interval, were applied to each sintered structure. The dielectric material was also printed with the DMC 11610 cartridge, heated to 32 °C. The printing resolution was set to 1016 dpi at 2 kHz, and the substrate was heated to 50 °C.

1.2. Synthesis of PANI ink

Polyaniline in the form of protonated emeraldine salt was prepared by the oxidation of 0.2 M aniline hydrochloride with 0.25 M ammonium persulfate at room temperature (**Figure 1**), as described in [10]. The temperature of the reaction mixture was monitored because the reaction is exothermic. The polymerization process lasted 15 minutes at a temperature of 37 °C. The resulting precipitate was filtered and washed with acetone and 0.2 M hydrochloric acid. Subsequently, it was dried on a hotplate at 60 °C for 2 hours, and then over silica gel in a desiccator for 24 hours. The PANI ink was prepared by mixing 2 mg of PANI in 1 mL xylene. A 0.5 μl aliquot of the prepared ink was deposited onto the interdigital electrode structures using a micropipette.

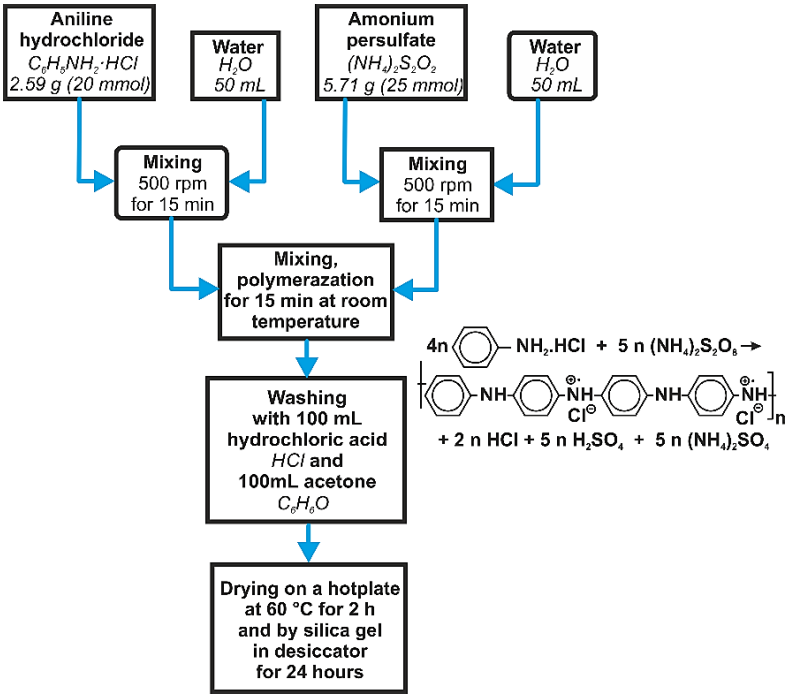

Figure 1 Flow diagram of the PANI synthesis

1.3. Sensor array fabrication

The prepared sensor array was initially divided into several individual parts, which were printed and characterized separately. Firstly, interdigital structures were printed and characterized, focusing on the appropriate resolution and the dimensions of the interdigital electrode structure. The results of the printed interdigital electrodes and dielectric mask are presented in [15]. Next, the heating elements were printed and characterized in terms of heat distribution and power consumption of the fabricated structures. The results of the prepared heaters are presented in [16]. Finally, heaters and IDE structures separated by a dielectric layer were printed and characterized. **Figure 2** shows the complete layout of the prepared sensor and each individual structure that was deposited.

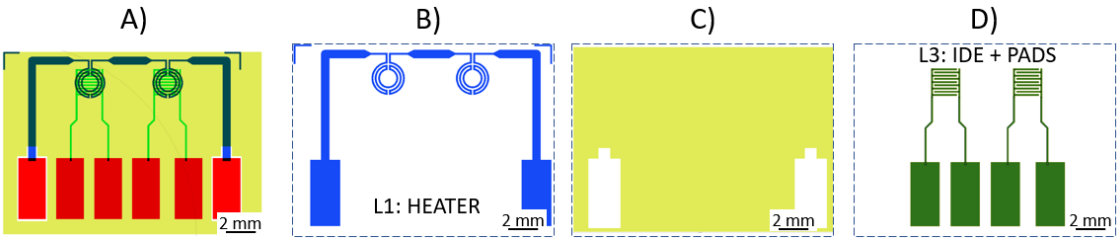

Figure 2 Layout of the prepared sensor multilayer structure: A) All layers combined together, B) First layer – heating structure printed with silver ink, C) Second layer – isolation printed with dielectric ink, D) Third layer – IDE structure and pads printed with silver ink.

The sensor fabrication process began with the heater layer, which was printed in two layers. This resulted in a thickness of 1 µm, according to previous results in [15].]. The heating structure and connecting paths were printed with a resolution of 1016 dpi using 2 nozzles to achieve high uniformity in each printed layer. The connecting pads were printed with the same resolution but with four nozzles. After drying for 20 hours, the structures were sintered using an IPL system. Subsequently, the isolation layers were printed with 15 nozzles. Four layers were deposited to ensure a flat and smooth surface. Each layer was cured with a UV LED immediately after printing. After completing the printing of the dielectric structure, it was further sintered in a laboratory oven for 30 minutes at 120 °C to complete the curing process of the polymer material.

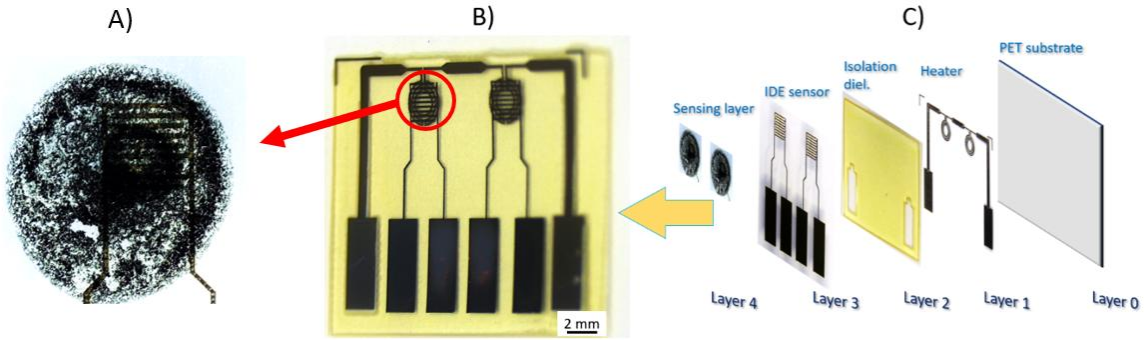

Figure 3 Platform of printed interdigital sensor array: A) PANI active layer drop cast on IDE structure, B) Complete sensor array with all layers, C) Exploded schema of the sensor array.

Before the deposition of the IDE structure, the surface of the insulation layer was prepared by plasma treatment. The structures were exposed to plasma etching with SF_6 gas for 30 seconds, with the parameters set as follows: ICP power 100 W and RF generator power 30 W. After the treatment, the IDE structure was immediately printed. Two layers of silver ink were deposited. However, due to the slow drying of the printed layer, the structures were transferred to a laboratory oven and dried at 60 °C for 30 minutes. After the first layer was completely dried, the second layer was printed. Following 20 hours of drying under room conditions, the structures were sintered using the IPL system under the same conditions as before. Finally, the sensing

material, PANI, was deposited using the drop-casting method. **Figure 3** shows the fully printed sensor with the deposited PANI layer and a schematic of the separately printed layers. The printed heater, IDE structure, and connecting pad with dimensions can be seen in **Figure 4**.

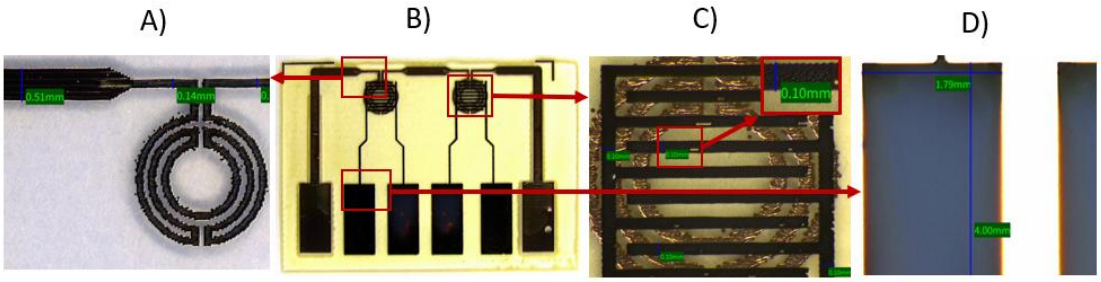

Figure 4 Details of printed sensor structures: A) Heating structure with dimensions, B) Completely printed sensor array, IDE with dimensions overprinted on dielectric and heating layers, C) Connecting pad with dimensions

2. RESULTS AND DISCUSSIONS

2.1. Temperature analysis and current-voltage characteristics of PANI

The temperature dependence of the prepared PANI layer is shown in **Figure 5a**. The temperature coefficient of resistance (TCR) of PANI was calculated in the temperature range from 23 °C to 80 °C using the formula $TCR = (\Delta R/R_0)/\Delta T$, where ΔR is the change in electrical resistance over a given temperature range, R_0 is the initial resistance, and ΔT is the temperature range. The TCR of PANI was found to be $-0.0023\ K^{-1}$. The temperature dependence of the polyaniline layers exhibits a negative temperature coefficient.

Figure 5b shows the current-voltage characteristics at various temperatures. These characteristics exhibit linear dependencies. The electrical resistivity of the PANI at 25 °C and 50 % relative humidity is 1934 Ω.

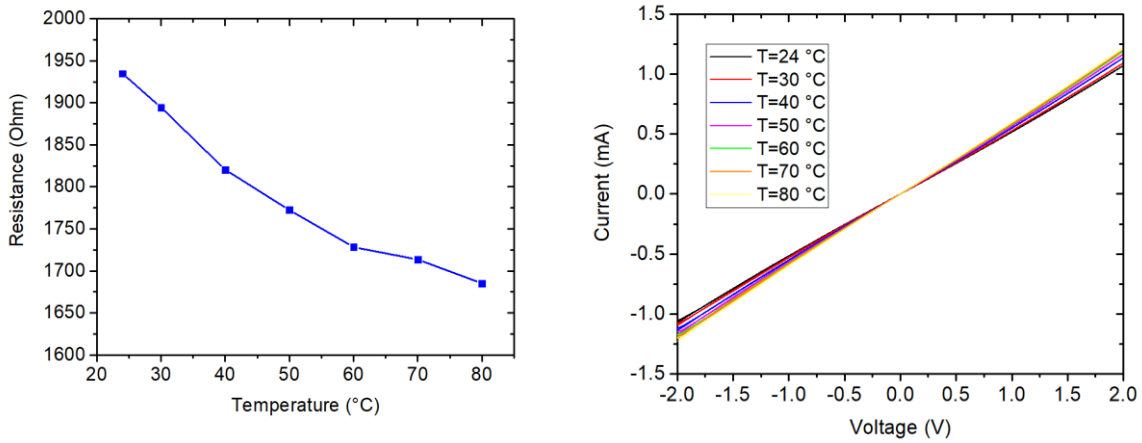

Figure 5 Temperature dependence of the PANI A) and current-voltage characteristics of PANI at various temperatures B).

2.2. Gas sensing analysis

The prepared sensor was tested in a custom-built apparatus for its response to ammonia (NH_3) and humidity (**Figure 6**). The exact concentration of ammonia was obtained by mixing it with the carrier gas. The desired humidity concentration was achieved by bubbling the carrier gas through water in the washer and then mixing

it with the carrier gas. The flow rate was maintained at 200 ml·min^{-1} using mass flow controllers. Synthetic air (SA - 21% O_2 and the remainder N_2) was used as the carrier gas and also served as the purge gas.

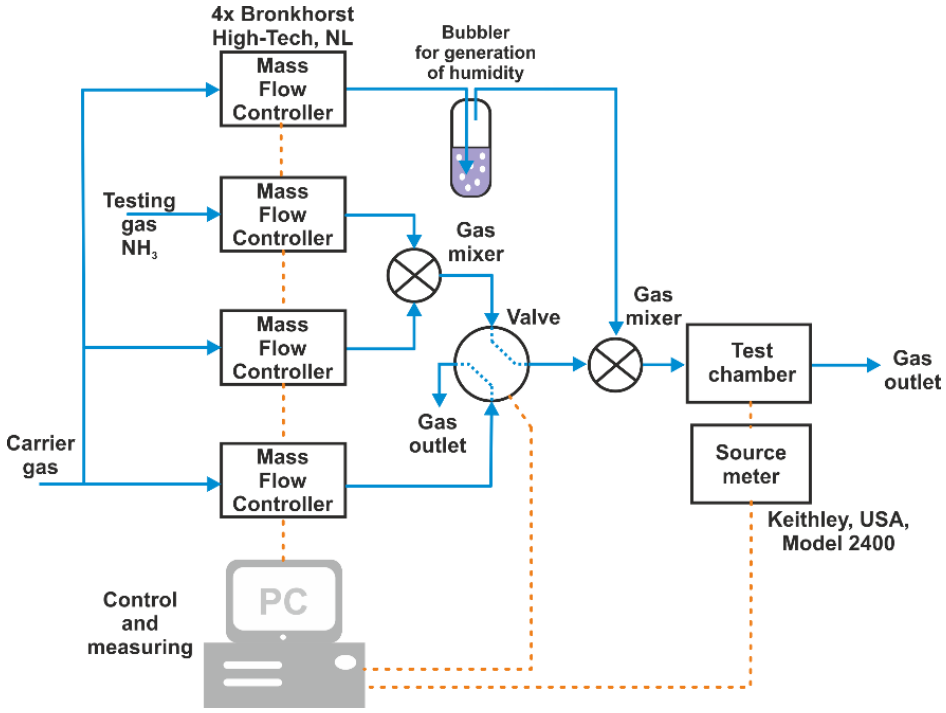

Figure 6 Schematic diagram of the customized sensing setup

The response of the PANI sensing layer was calculated using the formula for the relative resistance change, $\Delta R/R_0 = (R_s - R_0)/R_0$, where R_0 is the resistance at room temperature in synthetic air, and R_s is the resistance of the sensor in the presence of ammonia or humidity.

Figure 7 shows the response of the PANI layer to ammonia (12.5 ppm NH_3). The response of the sensor at room temperature and 50% relative humidity is shown in **Figure 7A**. Three cycles with the specified concentrations (10 minutes of exposure to the test gas, 10 minutes of synthetic air purging, flow rate 200 ml·min^{-1}) were performed during the testing with a constant voltage of 1 V.

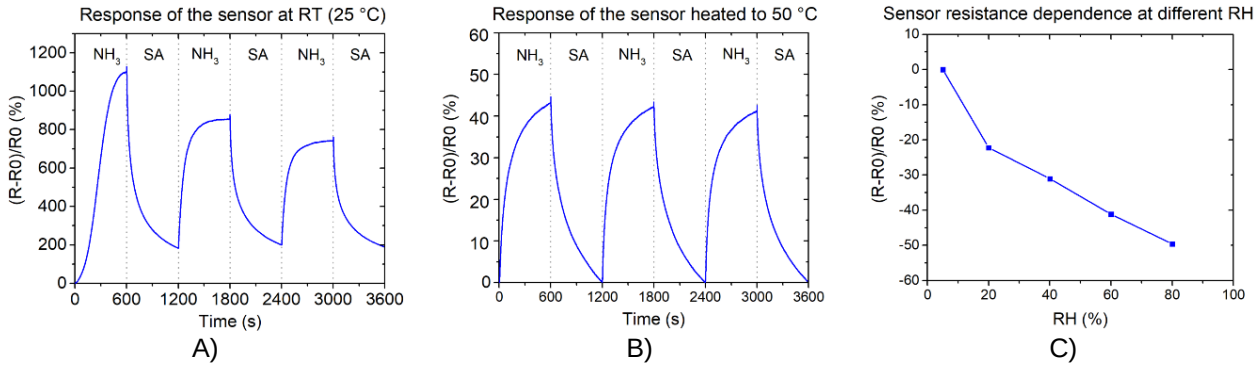

Figure 7 Gas characterization of the PANI layer: A) response to ammonia at room temperature, B) response to ammonia at 50 °C, C) dependence of PANI layer resistance on different levels of relative humidity.

When polyaniline is exposed to ammonia at room temperature, it shows a relatively high response but limited recovery and stability. When compared to a conventionally manufactured sensor, we found that our sensor achieved a response that was three times higher [10]. Increasing the operating temperature to 50 °C

(**Figure 7B**) results in a decrease in response but improved stability and better recovery of the sensor resistance to the initial value. The sensing mechanism was explained in [10].

The PANI layer exhibits significant sensitivity to humidity (**Figure 7C**). Electrical resistance decreases with increasing relative humidity.

3. CONCLUSION

In this work, a fully inkjet-printed gas sensor was fabricated. Silver ink was used to print the heating (bottom) and sensing (top) layers, and dielectric ink was used to print the isolation layer. The investigation demonstrated that the interdigital structure can be printed on the dielectric layer with expected dimensions. Moreover, the active layer of polyaniline was drop-cast, and its response to the test gas was examined. The results showed that the sensor exhibits a similar response to that of conventionally produced sensors. When the sensor was exposed to the test gas, it was confirmed that heating the sensing structure is desirable to achieve a stable response and effective recovery to the baseline. Additionally, the sensor exhibits significant sensitivity to varying levels of humidity. When the PANI layer was exposed to increasing temperatures, it showed a decrease in electrical resistivity. Both the thermal and humidity responses are comparable to those of conventionally produced sensors.

ACKNOWLEDGEMENTS

This work was supported by the Czech Science Foundation grant No. 22-04533S and by the Czech Technical University Student Grant No. SGS23/182/OHK3/3T/13.

REFERENCES

[1] S. H. HOSSEINI, R. A. KHALKHALI, and P. NOOR. “Study of polyaniline conducting/electroactive polymer as sensor for some agricultural phosphorus pesticides.” *Monatshefte für Chemie - Chem. Mon.* 2010, vol. 141, no. 10, pp. 1049–1053. Available from: https://doi.org/10.1007/s00706-010-0374-5.

[2] S. AKBAR, P. DUTTA, and C. LEE. “High-Temperature Ceramic Gas Sensors: A Review.” *Int. J. Appl. Ceram. Technol.* 2006, vol. 3, no. 4, pp. 302–311. Available from: https://doi.org/10.1111/j.1744-7402.2006.02084.x.

[3] E. BESCHER and J. D. MACKENZIE. “Hybrid organic-inorganic sensors.” *Mater. Sci. Eng. C*. Nov. 1998, vol. 6, no. 2–3, pp. 145–154. Available from: https://doi.org/10.1016/S0928-4931(98)00039-3.

[4] S. C. NAGARAJU, A. S. ROY, J. B. P. KUMAR, K. R. ANILKUMAR, and G. RAMAGOPAL. “Humidity Sensing Properties of Surface Modified Polyaniline Metal Oxide Composites.” *J. Eng.* 2014, pp. 1–8. Available from: https://doi.org/10.1155/2014/925020.

[5] B. J. FELDMAN, P. BURGMAYER, and R. W. MURRAY. “The potential dependence of electrical conductivity and chemical charge storage of poly(pyrrole) films on electrodes.” *J. Am. Chem. Soc.* 1985, vol. 107, no. 4, pp. 872–878. Available from: https://doi.org/10.1021/ja00290a024.

[6] H. KUZMANY, M. MEHRING, and S. ROTH. *Electronic Properties of Conjugated Polymers*, vol. 76. Berlin, Heidelberg: Springer Berlin Heidelberg, 1987.

[7] N. Li, J. Y. Lee, and L. H. Ong, “A polyaniline and Nafion composite film as a rechargeable battery,” *J. Appl. Electrochem.* 1992, vol. 22, no. 6, pp. 512–516. Available from: https://doi.org/10.1007/BF01024090.

[8] A. BOYLE, E. M. GENIÈS, and M. LAPKOWSKI. “Application of the electronic conducting polymers as sensors: Polyaniline in the solid state for detection of solvent vapours and polypyrrole for detection of biological ions in solutions.” *Synth. Met.* Jan. 1989, vol. 28, no. 1–2, pp. 769–774. Available from: https://doi.org/10.1016/0379-6779(89)90602-4.

[9] N. E. AGBOR, M. C. PETTY, and A. P. MONKMAN, “Polyaniline thin films for gas sensing,” *Sensors Actuators B Chem.* Oct. 1995, vol. 28, no. 3, pp. 173–179. Available from: https://doi.org/10.1016/0925-4005(95)01725-9.

[10] J. KROUTIL *et al.* “Performance Evaluation of Low-Cost Flexible Gas Sensor Array With Nanocomposite Polyaniline Films.” *IEEE Sens. J.* May 2018, vol. 18, no. 9, pp. 3759–3766. Available from: https://doi.org/10.1109/JSEN.2018.2811461.

[11] B. J. KANG, C. K. LEE, and J. H. OH. “All-inkjet-printed electrical components and circuit fabrication on a plastic substrate.” *Microelectron. Eng.* 2012. Available from: https://doi.org/10.1016/j.mee.2012.03.032.

[12] T. R. HEBNER, C. C. WU, D. MARCY, M. H. LU, and J. C. STURM. “Ink-jet printing of doped polymers for organic light emitting devices.” *Appl. Phys. Lett.* 1998. Available from: https://doi.org/10.1063/1.120807.

[13] S. B. FULLER, E. J. WILHELM, and J. M. JACOBSON. “Ink-jet printed nanoparticle microelectromechanical systems.” *J. Microelectromechanical Syst.* 2002. Available from: https://doi.org/10.1109/84.982863.

[14] L. GE *et al.* “A fully inkjet-printed disposable gas sensor matrix with molecularly imprinted gas-selective materials.” *npj Flex. Electron.* Jun. 2022, vol. 6, no. 1, p. 40. Available from: https://doi.org/10.1038/s41528-022-00168-6.

[15] V. POVOLNY, A. LAPOSA, J. KROUTIL, J. VOVES, M. DAVYDOVA, and P. HAZDRA. “Evaluation of printed interdigital electrodes array for chemo-resistive gas sensor application.” In *Proceedings 14th International Conference on Nanomaterials - Research & Application*, 2022, pp. 45–51. Available from: https://doi.org/10.37904/nanocon.2022.4588.

[16] V. POVOLNY, A. LAPOSA, J. KROUTIL, J. VOVES, P. ASHCHEULOV, and P. HAZDRA. “Evaluation of inkjet printed heaters array for chemo-resistive gas sensor.” 2023. Available from: https://doi.org/10.37904/nanocon.2023.4770.